

Published in final edited form as:

*Dent Mater.* 2013 August ; 29(8): . doi:10.1016/j.dental.2013.05.005.

## Synthesis of new antibacterial quaternary ammonium monomer for incorporation into CaP nanocomposite

Chenchen Zhou<sup>1,2</sup>, Michael D. Weir<sup>1</sup>, Ke Zhang<sup>1,3</sup>, Dongmei Deng<sup>4</sup>, Lei Cheng<sup>1,2</sup>, and Hockin H. K. Xu<sup>1,5,6</sup>

<sup>1</sup>Biomaterials & Tissue Engineering Division, Department of Endodontics, Prosthodontics and Operative Dentistry, University of Maryland School of Dentistry, Baltimore, MD 21201, USA

<sup>2</sup>State Key Laboratory of Oral Diseases, West China School of Stomatology, Sichuan University, Chengdu, China <sup>3</sup>Department of Orthodontics, School of Stomatology, Capital Medical University, Beijing, China <sup>4</sup>Department of Cariology, Endodontology and Pedodontology, Academic Centre for Dentistry, Amsterdam, The Netherlands <sup>5</sup>Center for Stem Cell Biology & Regenerative Medicine, University of Maryland School of Medicine, Baltimore, MD 21201, USA <sup>6</sup>Department of Mechanical Engineering, University of Maryland, Baltimore County, MD 21250

### Abstract

**Objectives**—Composites are the principal material for tooth cavity restorations due to their esthetics and direct-filling capabilities. However, composites accumulate biofilms in vivo, and secondary caries due to biofilm acids is the main cause of restoration failure. The objectives of this study were to: (1) synthesize new antibacterial monomers; and (2) develop nanocomposite containing nanoparticles of amorphous calcium phosphate (NACP) and antibacterial monomer.

**Methods**—Two new antibacterial monomers were synthesized: dimethylaminohexane methacrylate (DMAHM) with a carbon chain length of 6, and dimethylaminododecyl methacrylate (DMADDM) with a chain length of 12. A spray-drying technique was used to make NACP. DMADDM was incorporated into NACP nanocomposite at mass fractions of 0%, 0.75%, 1.5%, 2.25% and 3%. A flexural test was used to measure composite strength and elastic modulus. A dental plaque microcosm biofilm model with human saliva as inoculum was used to measure viability, metabolic activity, and lactic acid production of biofilms on composites.

**Results**—The new DMAHM was more potent than a previous quaternary ammonium dimethacrylate (QADM). DMADDM was much more strongly antibacterial than DMAHM. The new DMADDM-NACP nanocomposite had strength similar to that of composite control ( $p > 0.1$ ). At 3% DMADDM in the composite, the metabolic activity of adherent biofilms was reduced to 5% of that on composite control. Lactic acid production by biofilms on composite containing 3% DMADDM was reduced to only 1% of that on composite control. Biofilm colony-forming unit (CFU) counts on composite with 3% DMADDM were reduced by 2-3 orders of magnitude.

---

© 2004 Academy of Dental Materials. Published by Elsevier Ltd. All rights reserved.

Correspondence: Dr. Hockin H. K. Xu, Professor, Director of Biomaterials & Tissue Engineering Division, Department of Endodontics, University of Maryland Dental School, Baltimore, MD 21201 (hxu@umaryland.edu), and Dr. Lei Cheng, Associate Professor, West China School of Stomatology, Sichuan University, China (chengleidentist@163.com).

**Publisher's Disclaimer:** This is a PDF file of an unedited manuscript that has been accepted for publication. As a service to our customers we are providing this early version of the manuscript. The manuscript will undergo copyediting, typesetting, and review of the resulting proof before it is published in its final citable form. Please note that during the production process errors may be discovered which could affect the content, and all legal disclaimers that apply to the journal pertain.

**Significance**—New antibacterial monomers were synthesized, and the carbon chain length had a strong effect on antibacterial efficacy. The new DMADDM-NACP nanocomposite possessed potent anti-biofilm activity without compromising load-bearing properties, and is promising for antibacterial and remineralizing dental restorations to inhibit secondary caries.

### Keywords

Antibacterial nanocomposite; calcium phosphate nanoparticles; quaternary ammonium; human saliva microcosm biofilm; mechanical properties; caries inhibition

## 1. Introduction

Dental caries remains a prevalent problem worldwide [1-3]. The longevity of tooth cavity restorations is limited, with half of all restorations failing in less than 10 years, mainly due to secondary caries and fracture [4-7]. Replacing the failed restorations accounts for 50-70% of all restorations performed [8,9]. This is costly, considering that the annual cost for tooth cavity restorations in the U.S. was approximately \$46 billion in 2005 [10]. Furthermore, the need is rapidly increasing as baby boomers enter into retirement, with increases in life expectancy as well as tooth retention in seniors [11]. Due to their esthetics and direct-filling capabilities, resin composites are the principal material for cavity restorations [6,7,12-19]. Improvements in filler particles and matrix polymers have significantly enhanced the composite properties [20-23]. Nonetheless, one major drawback remains: Composites tend to accumulate more biofilms/plaques than other restoratives in vivo [24,25]. Acidogenic bacteria such as *Streptococcus mutans* (*S. mutans*) and their biofilms, upon exposure to fermentable carbohydrates, produce acids that lead to caries [26]. Therefore, efforts were made to develop antibacterial resins [27-32]. Quaternary ammonium methacrylates (QAMs) were synthesized with antibacterial activities [33-36]. Indeed, 12-methacryloyloxydodecylpyridinium bromide (MDPB) and other antibacterial resins decreased the growth of oral bacteria [32-36].

Calcium phosphate (CaP) biomaterials are important due to their bioactivity, biocompatibility and similarity to the minerals in teeth and bones [37-39]. Resin composites with CaP fillers released Ca and P ions and remineralized tooth lesions [37-39]. However, traditional CaP composites contained CaP particles with sizes of 1-55  $\mu\text{m}$  [37-39], with relatively low mechanical properties that were “inadequate to make these composites acceptable as bulk restoratives” [40]. Furthermore, the CaP resin composites had no antibacterial activity.

Novel nanoparticles of CaP were synthesized and mixed into composites with the release of Ca and P ions [41-43]. Composites with nanoparticles of amorphous calcium phosphate (NACP) neutralized acid attacks, while commercial controls failed to neutralize the acids [44]. Glass filler reinforcement yielded photo-cured NACP nanocomposite with Ca and P ion release comparable to, and mechanical properties 2-3 fold of, traditional CaP composites [45]. In 2 years of water-aging, mechanical properties of NACP nanocomposite matched those of commercial non-remineralizing composite control [46]. NACP nanocomposite reduced secondary caries in enamel in a human in situ study [47], and remineralized tooth lesions in vitro [48]. Recently, NACP were combined with a quaternary ammonium dimethacrylate (QADM) to develop nanocomposite with a combination of remineralizing and antibacterial capabilities [49,50]. In the present study, a new quaternary ammonium monomer, dimethylaminododecyl methacrylate (DMADDM) was synthesized, which had a much greater antibacterial potency than the previously-used QADM.

Therefore, the objectives of this study were to synthesize new antibacterial monomer DMADDM, and develop nanocomposite containing NACP for remineralization and DMADDM for potent antibacterial activity for the first time. The following hypotheses were tested: (1) The new antibacterial monomer DMADDM would have lower minimum inhibition concentration (MIC) and minimum bactericidal concentration (MBC) than the former QADM; (2) DMADDM could be incorporated into NACP nanocomposite without decreasing the composite mechanical properties; (3) DMADDM-NACP nanocomposite would significantly reduce dental plaque microcosm biofilm growth, metabolic activity, and lactic acid production.

## 2. Materials and methods

### 2.1. Synthesis of new quaternary ammonium methacrylates (QAMs)

A modified Menshutkin reaction approach was used to synthesize the new QAMs. This method uses a tertiary amine group to react with an organo-halide, as described in previous studies [32,49]. A benefit of this reaction is that the reaction products are generated at virtually quantitative amounts and require minimal purification [32]. In the present study, 2-bromoethyl methacrylate (BEMA) was the organo-halide. N,N-dimethylaminohexane (DMAH) and 1-(dimethylamino)docecane (DMAD) were the two tertiary amines.

The scheme of synthesis of dimethylaminohexane methacrylate (DMAHM) is shown in Fig. 1A. Ten mmol of DMAH (Tokyo Chemical Industry, Tokyo, Japan), 10 mmol of BEMA (Monomer-Polymer and Dajac Labs, Trevoze, PA), and 3 g of ethanol were added to a 20 mL scintillation vial with a magnetic stir bar. The vial was capped and stirred at 70 °C for 24 h. After the reaction was complete, the ethanol solvent was removed via evaporation at room temperature over several days. This yielded DMAHM as a clear liquid.

The scheme of synthesis of dimethylaminododecyl methacrylate (DMADDM) is shown in Fig. 1B. In a 20 mL scintillation vials were added 10 mmol of DMAD (Tokyo Chemical Industry), 10 mmol of BEMA, and 3 g of ethanol. A magnetic stir bar was added, and the vial was capped and stirred at 70 °C for 24 h. After the reaction was complete, the solvent was removed via evaporation. The number of the alkyl chain length units was 6 for DMAHM and 12 for DMADDM (Fig. 1).

To characterize the reaction products, Fourier transform infrared spectroscopy (FTIR, Nicolet 6700, Thermo Scientific, Waltham, MA) was used. FTIR spectra of the starting materials and the viscous products were collected between two KBr windows in the 4000  $\text{cm}^{-1}$  to 400  $\text{cm}^{-1}$  region with 128 scans at 4  $\text{cm}^{-1}$  resolution [32]. Water and  $\text{CO}_2$  bands were removed from all spectra by subtraction.  $^1\text{H}$  NMR spectra (GSX 270, JEOL, Peabody, MA) of the starting materials and products were taken in deuterated chloroform at a concentration of approximately 3%. All spectra were run at room temperature, 15 Hz sample spinning, 45° tip angle for the observation pulse, and a 10 s recycle delay, for 64 scans [32].

### 2.2. Minimum Inhibitory Concentration (MIC) and Bactericidal Concentration (MBC)

MIC is the lowest concentration of an antimicrobial agent that will inhibit the visible growth of a microorganism [51,52]. When the antibacterial agent is added into a bacterial solution at the MIC, not all the bacteria are killed, but the concentration of bacteria is so low that the solution appears clear without turbidity [52]. When the MBC of an antibacterial agent is used in a bacterial solution, all the bacteria will be killed; if this solution is placed on agar plates, there will be no bacteria colonies after incubation. MIC and MBC were measured using *S. mutans* (ATCC 700610, UA159, American Type Culture, Manassas, VA). The use of *S. mutans* was approved by the University of Maryland. *S. mutans* is a cariogenic, aerotolerant anaerobic bacterium and the primary causative agent of dental caries [26]. MIC

and MBC were determined via serial microdilution assays [51,52]. Unpolymerized DMAHM or DMADDM monomer was dissolved in brain heart infusion (BHI) broth (BD, Franklin Lakes, NJ) to give a final concentration of 200 mg/mL. From these starting solutions, serial two fold dilutions were made into 1 mL volumes of BHI broth. Fifteen  $\mu\text{L}$  of stock *S. mutans* was added to 15 mL of BHI broth with 0.2% sucrose and incubated at 37 °C with 5%  $\text{CO}_2$ . Overnight cultures of *S. mutans* were adjusted to  $2 \times 10^6$  CFU/mL with BHI broth, and 50  $\mu\text{L}$  of inocula was added to each well of a 96-well plate containing 50  $\mu\text{L}$  of a series of antibacterial monomer dilution broths. BHI broth with  $1 \times 10^6$  CFU/mL bacteria suspension without antibacterial agent served as negative control. Chlorhexidine diacetate (CHX) (Sigma, St. Louis, MO) served as positive control. The previously-synthesized QADM [32,49] served as an antibacterial monomer control. After incubation at 37 °C in 5%  $\text{CO}_2$  for 48 h, the wells were read for turbidity, referenced by the negative and positive control wells. MIC was determined as the endpoint (the well with the lowest antibacterial agent concentration) where no turbidity could be detected with respect to the controls [52]. To determine MBC, an aliquot of 50  $\mu\text{L}$  from each well without turbidity was inoculated on BHI agar plates and incubated at 37 °C in 5%  $\text{CO}_2$  for 48 h. MBC was determined as the lowest concentration of antibacterial agent that produced no colonies on the plate. The tests were performed in triplicate [52].

### 2.3. Processing of DMADDM-NACP nanocomposite

A spray-drying technique as described previously [53] was used to make NACP ( $\text{Ca}_3[\text{PO}_4]_2$ ). Calcium carbonate ( $\text{CaCO}_3$ , Fisher, Fair Lawn, NJ) and dicalcium phosphate anhydrous ( $\text{CaHPO}_4$ , Baker Chemical, Phillipsburg, NJ) were dissolved into an acetic acid solution to obtain final Ca and P ionic concentrations of 8 mmol/L and 5.333 mmol/L, respectively. This resulted in a Ca/P molar ratio of 1.5, the same as that for ACP. This solution was sprayed into a heated chamber, and an electrostatic precipitator (AirQuality, Minneapolis, MN) was used to collect the dried particles. This method produced NACP with a mean particle size of 116 nm, as measured in a previous study [45].

Because Section 2.2 showed that DMADDM had a much greater antibacterial potency than DMAHM and QADM, DMADDM was used for incorporation into the NACP nanocomposite to obtain antibacterial properties. BisGMA (bisphenol glycidyl dimethacrylate) and TEGDMA (triethylene glycol dimethacrylate) (Esstech, Essington, PA) were mixed at a mass ratio = 1:1, and rendered light-curable with 0.2% camphorquinone and 0.8% ethyl 4-N,N-dimethylaminobenzoate (mass fractions). DMADDM was mixed with the photo-activated BisGMA-TEGDMA resin at the following DMADDM/(BisGMA-TEGDMA + DMADDM) mass fractions: 0%, 2.5%, 5%, 7.5% and 10%, yielding five groups of resin, respectively. The 10% mass fraction followed previous studies [54,56]. The other mass fractions enabled the investigation of the relationship between DMADDM mass fraction and antibacterial efficacy. A dental barium boroaluminosilicate glass of a median particle size of 1.4  $\mu\text{m}$  (Caulk/Dentsply, Milford, DE) was silanized with 4% 3-methacryloxypropyltrimethoxysilane and 2% n-propylamine [45]. The NACP and glass particles were mixed into each resin, at the same filler level of 70% by mass, with 20% of NACP and 50% of glass [45]. Because the resin mass fraction was 30% in the composite, the five DMADDM mass fractions in the composite were 0%, 0.75%, 1.5%, 2.25% and 3%, respectively.

Six composites were tested: Five NACP nanocomposites at the five DMADDM mass fractions described above, and a commercial control composite. Renamel (Cosmedent, Chicago, IL) served as a control composite. It consisted of nanofillers of 20 - 40 nm in size, at 60% filler level in a multifunctional methacrylate ester resin. For mechanical testing, each paste was placed into rectangular molds of  $2 \times 2 \times 25$  mm. For biofilm experiments, each paste

was placed into disk molds of 9 mm in diameter and 2 mm in thickness. The specimens were photo-cured (Triad 2000, Dentsply, York, PA) for 1 min on each side. The specimens were then incubated in distilled water at 37 °C for 24 hours prior to mechanical or biofilm testing.

#### 2.4. Mechanical testing

A computer-controlled Universal Testing Machine (5500R, MTS, Cary, NC) was used to fracture the specimens in three-point flexure using a span of 10 mm and a crosshead speed of 1 mm/min. Flexural strength  $S$  was measured as:  $S = 3P_{\max}L/(2bh^2)$ , where  $P_{\max}$  is the load-at-failure,  $L$  is span,  $b$  is specimen width and  $h$  is specimen thickness. Elastic modulus  $E$  was measured as:  $E = (P/d)(L^3/[4bh^3])$ , where load  $P$  divided by displacement  $d$  is the slope in the linear elastic region of the load-displacement curve. The specimens were taken out of the water and fractured within several minutes while still being wet [49].

#### 2.5. Dental plaque microcosm biofilm and live/dead assay

The use of the dental plaque microcosm biofilm model with human saliva as inoculum was approved by the University of Maryland. Saliva was collected from a healthy adult donor following a previous study [54]. The donor had natural dentition without active caries or periopathology, and without the use of antibiotics within the last 3 months. The donor did not brush teeth for 24 h and abstained from food or drink intake for at least 2 h prior to donating saliva [54]. Stimulated saliva was collected during parafilm chewing and kept on ice. The saliva was diluted in sterile glycerol to a concentration of 70 % saliva and 30% glycerol [54]. The saliva-glycerol stock was added, with 1:50 final dilution, into the growth medium as inoculum. The growth medium was the McBain artificial saliva medium, which contained mucin (type II, porcine, gastric) at a concentration of 2.5 g/L; bacteriological peptone, 2.0 g/L; tryptone, 2.0 g/L; yeast extract, 1.0 g/L; NaCl, 0.35 g/L, KCl, 0.2 g/L; CaCl<sub>2</sub>, 0.2 g/L; cysteine hydrochloride, 0.1 g/L; haemin, 0.001 g/L; vitamin K<sub>1</sub>, 0.0002 g/L, at pH 7 [55]. A 1.5 mL of inoculum was measured to contain total microorganisms of  $(2.4 \pm 0.2) \times 10^6$  CFU, which included total streptococci of  $(1.0 \pm 0.1) \times 10^5$  CFU, and mutans streptococci of  $(3.3 \pm 0.8) \times 10^4$  CFU. The composite disks were sterilized in ethylene oxide (Anprolene AN 74i, Andersen, Haw River, NC). The 1.5 mL of inoculum was added to each well of 24-well plates with a composite disk, and incubated in 5% CO<sub>2</sub> at 37 °C for 8 h.

The disks were then transferred to new 24-well plates filled with fresh medium and incubated. After 16 h, the disks were transferred to new 24-well plates with fresh medium and incubated for 24 h. This totaled 48 h of incubation, which was shown to be adequate to form dental plaque microcosm biofilms on resins [54,56].

After 48 h of growth, the microcosm biofilms adherent on the disks were gently washed three times with phosphate buffered saline (PBS), and then stained using the BacLight live/dead bacterial viability kit (Molecular Probes, Eugene, OR) [54,56]. Live bacteria were stained with Syto 9 to produce a green fluorescence, and bacteria with compromised membranes were stained with propidium iodide to produce a red fluorescence. The stained disks were examined using a confocal laser scanning microscopy (CLSM 510, Carl Zeiss, Thornwood, NY).

#### 2.6. MTT assays

MTT (3-(4,5-Dimethylthiazol-2-yl)-2,5-diphenyltetrazolium bromide) assay was performed according to previous studies [32,49]. It is a colorimetric method that measures the enzymatic reduction of MTT, a yellow tetrazole, to formazan. Briefly, disks with 48-h biofilms were rinsed with PBS and transferred to 24 well plates. Then, 1 mL of MTT dye (0.5 mg/mL MTT in PBS) was added to each well and incubated for 1 h. The disks were transferred to new 24-well plates, 1 mL of dimethyl sulfoxide (DMSO) was added to



solubilize the formazan crystals, and the plate was incubated for 20 min in the dark. Then, 200  $\mu\text{L}$  of the DMSO solution from each well was transferred to a 96-well plate, and the absorbance at 540 nm was measured via a microplate reader (SpectraMax M5, Molecular Devices, Sunnyvale, CA) [49].

## 2.7. Lactic acid production and CFU counts

Composite disks with 48-h biofilms were rinsed in cysteine peptone water (CPW) to remove the loose bacteria. Each disk was placed in a new 24-well plate and 1.5 mL of buffered peptone water (BPW) supplemented with 0.2% sucrose [49]. The samples were incubated in 5%  $\text{CO}_2$  at 37 °C for 3 h to allow the biofilms to produce acid. The BPW solutions were then stored for lactate analysis. Lactate concentrations were determined using an enzymatic (lactate dehydrogenase) method according to previous studies [49,54]. The microplate reader was used to measure the absorbance at 340 nm for the collected BPW solutions. Standard curves were prepared using a lactic acid standard (Supelco Analytical, Bellefonte, PA) [49,54].

Composite disks with 2-day biofilms were transferred into tubes with 2 mL CPW, and the biofilms were harvested by sonication (3510R-MTH, Branson, Danbury, CT) for 5 minutes, followed by vortexing at 2400 rpm for 30 seconds using a vortex mixer (Fisher Scientific, Pittsburgh, PA). Three types of agar plates were used to assess the microorganism viability after serial dilution in CPW: Mitis salivarius agar (MSA) culture plates, containing 15% sucrose, to determine total streptococci [57]; MSA agar culture plates plus 0.2 units of bacitracin per mL, to determine mutans streptococci [58]; and Tryptic Soy Blood Agar culture plates to determine total microorganisms [54].

One-way analysis of variance (ANOVA) was performed to detect the significant effects of the variables. Tukey's multiple comparison test was used at a p value of 0.05.

## 3. Results

As shown in Fig. 2, the characterization of DMAHM and DMADDM using FTIR indicated that the Menshutkin reaction was successful. The infrared spectroscopy showed the disappearance of C-Br and tertiary amine groups, and the appearance of quaternary ammonium group that resulted from the reaction. In Fig. 2A, FTIR showed that the C-Br absorption bands from BEMA ( $575\text{ cm}^{-1}$ ,  $512\text{ cm}^{-1}$ ) in curve 1 and the  $(\text{CH}_3)_2\text{N}$ - bands ( $2822\text{ cm}^{-1}$ ,  $2771\text{ cm}^{-1}$ ) from DMAH in curve 2 were not detected in curve 3. This indicated that the bromine group in BEMA successfully reacted with the amine group in DMHA to form the quaternary ammonium group. The appearance in curve 3 of the  $\text{NR}_4^+$  peak corresponded to the formation of the quaternary ammonium group and, hence, DMAHM was successfully synthesized. Similarly, Fig. 2B showed the synthesis of DMADDM from the reaction of BEMA and DMAD. The structures of DMAHM and DMADDM were confirmed via  $^1\text{H}$ NMR by assigning peaks to the respective alkyl group of each monomer. The peak assignments for the  $^1\text{H}$  NMR [ (ppm)] of DMADDM were: 3.43 (6H, s,  $\text{CH}_3\text{N}$ ), 5.43, 6.01 (2H, s,  $\text{CH}_2\text{CCH}_3\text{C}$ ), 4.56 (4H, s,  $\text{CH}_2\text{CH}_2\text{N}$ ), 4.18 (3H, s,  $\text{CH}_3\text{CH}_2\text{O}$ ), and 3.76 (25H, m,  $\text{CH}_3(\text{CH}_2)_{11}\text{N}$ ), which confirmed the structure of DMADDM.

The MIC and MBC values of the antibacterial agents against *S. mutans* are listed in Table 1. A lower concentration of the antibacterial agent needed to inhibit the bacteria indicates a higher antibacterial potency. The new DMAHM with an alkyl chain length of 6 was more potent than the previously-synthesized QADM. In dramatic contrast, the new DMADDM with an alkyl chain length of 12 was much more strongly antibacterial than DMAHM. The

MIC and MBC of DMADDM was more than two orders of magnitude lower than those of DMAHM, and approached those of the CHX control.

Fig. 3 plots (A) flexural strength, and (B) elastic modulus of the composites (mean  $\pm$  sd; n = 6). The NACP nanocomposite with various DMADDM mass fractions had strengths similar to that of the commercial composite control, which was not antibacterial and had no Ca and P ion release ( $p > 0.1$ ). The elastic moduli of DMADDM-NACP nanocomposites were also similar to those of the NACP nanocomposite without DMADDM and the composite control ( $p > 0.1$ ).

Representative CLSM images of live/dead biofilms adherent on the composites are shown in Fig. 4. Biofilms on composite control and NACP nanocomposite without DMADDM had primarily live bacteria. Increasing the DMADDM mass fraction in the nanocomposite resulted in much more red/yellow/orange staining, indicating that the DMADDM-containing nanocomposites effectively inhibited the biofilm growth. These results also indicate that NACP was not antibacterial, and DMADDM was responsible for the antibacterial activity.

Fig. 5 plots (A) the MTT assay, and (B) lactic acid production of biofilms adherent on the composites. Each values is mean  $\pm$  sd (n = 6). In (A), the biofilms on composite control and NACP + 0% DMADDM had a similar metabolic activity ( $p > 0.1$ ). Increasing the DMADDM mass fraction significantly decreased the metabolic activity of biofilms ( $p < 0.05$ ). At 3% DMADDM in the composite, the metabolic activity was approximately 5% of that on composite control. In (B), the biofilms on composite control produced the most acid, similar to that on NACP + 0% DMADDM. With increasing DMADDM mass fraction, the lactic acid production monotonically decreased ( $p < 0.05$ ). The lactic acid production by biofilms on NACP + 3% DMADDM was about 1% of that on the commercial composite control.

Fig. 6 plots the CFU counts for: (A) Total microorganisms, (B) total streptococci, and (C) mutans streptococci (mean  $\pm$  sd; n = 6). The composite control had the highest CFU counts. All three CFU counts showed a similar decreasing trend with increasing DMADDM mass fraction in NACP nanocomposite ( $p < 0.05$ ). Compared to the control composite, all three CFU counts on NACP + 3% DMADDM were reduced by 2-3 orders of magnitude.

#### 4. Discussion

QAMs can be copolymerized with the resin by forming a covalent bonding with the polymer network, and hence are immobilized in the composite and not released or lost over time [27,28]. Therefore, a durable antibacterial activity can be achieved for the composite. Previous study showed that resins containing MDPB maintained the antibacterial effect after water-aging for 3 months [59]. Quaternary ammonium bromides and chlorides were incorporated into a glass ionomer cement, yielding long-lasting antimicrobial capabilities [30]. Other studies synthesized QADM and incorporated it into resins, yielding effective antibacterial activities [32,50]. While the detailed antimicrobial mechanism is yet to be established, it was suggested that quaternary ammonium agents can cause bacteria lysis by binding to cell membrane and causing cytoplasmic leakage [60]. When the negatively charged bacterial cell contacts the positively charged ( $N^+$ ) sites of the quaternary ammonium, the electric balance of the cell membrane could be disturbed, and the bacterium could explode under its own osmotic pressure [61]. The long cationic polymers can penetrate bacterial cells to disrupt the membrane, like a needle bursting a balloon [62,63]. Therefore, the carbon chain length is an important parameter for the antibacterial monomer, and needs to be long enough to penetrate the cell membrane [62,63].

The present study developed DMAHM with a chain length of 6 and DMADDM with a chain length of 12 for the first time. Regarding the purity of the synthesized monomers, the primary contaminants would most likely be unreacted BEMA, DMAH and DMAD. Care was taken to remove all of these potential impurities via evaporation in vacuum prior to use. The FTIR data indicates that BEMA, DMAH and DMAD were not present in the final product (the C-Br peak and the tertiary amine peak of the DMAH and DMAD were not detected in the FTIR spectrum of the final product). Furthermore, as a preliminary test, a high performance liquid chromatography (HPLC, Beckman Coulter, Fullerton, CA) was used to measure monomer leachout from the cured resin disks containing 10% DMADDM, which yielded no measurable concentration of unreacted BEMA, DMAH and DMAD elution from the cured disks. This indicates that the DMADDM obtained was relatively pure with negligible impurities. However, further study is needed to measure the monomer purity, perhaps via gas chromatography-mass spectrometry. Increasing the chain length from 6 to 12 reduced the MIC and MBC by more than two orders of magnitude. Both new monomers had much stronger antibacterial potency than the previously-reported QADM [32,49,50]. QADM has a carbon chain length of 2, although it is a dimethacrylate with a different chemical structure from the DMADDM and DMAHM system. However, the results of the present study clearly indicated the strong effect of increasing the carbon chain length on increasing the antibacterial potency of the monomers. It is interesting to compare the MIC (6.1 µg/mL) and MBC (12.21 µg/mL) of DMADDM to MDPB. This is because a MDPB-containing bonding agent was reported as “The world’s first antibacterial adhesive system” [28], and MDPB has been extensively studied [27,28,33,34,51,59]. The MIC and MBC of MDPB against *S. mutans* were reported to be 15.6 µg/mL [59] and 62.5 µg/mL [64], respectively. The MIC and MBC of the new DMADDM of the present study were lower by 3-5 folds compared to those of MDPB, indicating that DMADDM might be more strongly antibacterial. It should be noted that data from different papers may not be directly comparable. In addition, while DMADDM had a chain length of 12, future study should investigate if further increasing the chain length from 12 to 14 or 16 would result in a further increase in the antibacterial potency.

Several previous studies developed dental composites containing antibacterial monomers. Imazato et al. incorporated MDPB into a composite which reduced the glucan synthesis and growth of *S. mutans* on its surface [27,59]. The incorporation of MDPB had no significant effect on the mechanical properties or polymerization conversion of the composite [59]. Xu et al. synthesized antibacterial fluoride-releasing composites [4]. Their studies indicated that the composite containing 3% of N-benzyl-11-(methacryloyloxy)-N,N-dimethylundecan-1-aminium fluoride had a significant effect against *S. mutans* biofilm without adverse effects on its physical and mechanical properties [35]. Beyth et al. incorporated quaternary ammonium polyethylenimine (QPEI) nanoparticles into composite, which exhibited a broad spectrum antibacterial activity against salivary bacteria in vivo [65]. Weng et al. synthesized a furanone-containing antibacterial composite, which showed 16-68% reduction in *S. mutans* viability [36]. While these previous studies are meritorious, the present study is unique in that the new nanocomposite not only possessed strong antibacterial properties, but also contained NACP for Ca and P ion release and remineralization capability.

Recent studies incorporated QADM and nanoparticles of silver (NAg) into nanostructured composites [49,50]. Mechanically-strong nanocomposite containing QADM, NAg and NACP decreased the titer counts of adherent *S. mutans* biofilms compared to a control composite [49]. The antibacterial properties of NACP nanocomposite containing QADM were maintained after water-aging for 180 days, without significant decrease over time [50]. The present study demonstrated that the new DMADDM could be incorporated into the NACP nanocomposite to impart a strong antibacterial activity without compromising mechanical properties. This indicates the versatility of incorporating various types of



antibacterial monomers into the NACP nanocomposite, and the miscibility and compatibility of the antibacterial monomers with NACP nanocomposite. It is interesting to compare the DMADDM nanocomposite of the present study with the previous QADM nanocomposite tested by the same operator using the same procedures [50]. The previous QADM nanocomposite reduced the MTT metabolic activity by 2-fold, compared to the same control composite [50]. The present study using DMADDM reduced the MTT by 20-fold. In addition, the previous QADM nanocomposite reduced the lactic acid production by 2-fold [50]; the present study using DMADDM reduced lactic acid by 2 orders of magnitude. Furthermore, the previous QADM nanocomposite reduced the biofilm CFU counts by 3-fold [50]; the present study using DMADDM reduced the biofilm CFU by 2-3 orders of magnitude. Therefore, the new DMADDM-NACP nanocomposite represents a substantial improvement over previous antibacterial dental composites. Another issue that should be pointed out is that the present study used the McBain artificial saliva medium, which reflects the gross composition of salivary secretions such as mucin [55]. A recent study investigated the effects of salivary pellicles on the antibacterial properties of resin [66]. When cultured in Brain Heart Infusion (BHI) medium which has no salivary proteins, pre-coating the resin specimens with salivary pellicles before bacteria inoculation significantly reduced the antibacterial activity. In contrast, when cultured in McBain medium, there was no significant difference in the antibacterial activity whether the resin specimens were pre-coated with salivary pellicles or not [66]. These results suggested that the McBain artificial saliva medium yielded medium-derived pellicles on the resin surfaces, which provided attenuating effects on biofilms similar to salivary pellicles [66]. Therefore, the present study used the McBain artificial saliva medium to test the antibacterial efficacy of the DMADDM nanocomposite, which included the salivary attenuating effect on the anti-biofilm efficacy.

It should be noted that the DMADDM-NACP nanocomposite is not only antibacterial, but also has Ca and P ion release and remineralization capabilities. The present study focused on monomer synthesis, composite processing and anti-biofilm properties, without investigating the ion release and remineralization properties. Several recent studies measured the ion release and remineralization properties of NACP nanocomposites. The NACP nanocomposite was “smart” and increased the Ca and P ion release at a cariogenic pH of 4, when these ions would be most needed to inhibit caries [45]. When immersed in a lactic acid solution of pH 4, the NACP nanocomposite neutralized the acid attack and increased the pH from 4 to a safe pH of 6 [44]. NACP nanocomposite achieved much higher remineralization of enamel lesions, compared to a commercial fluoride-releasing composite [48]. In a human in situ study, the enamel lesion at the margins around NACP nanocomposite in vivo was only half of the lesion around a control composite [47]. The NACP nanocomposite in these previous studies [47,48] had no antibacterial agents. It is anticipated that the new DMADDM-NACP nanocomposite, with a combination of antibacterial and remineralization capabilities, would be even more effective for caries-inhibiting restorations, which warrants further study.

## 5. Conclusions

New antibacterial monomers DMAHM and DMADDM were synthesized, and the carbon chain length was shown to have a strong effect on antibacterial efficacy. DMADDM with a chain length of 12 was much more strongly antibacterial than DMAHM with a chain length of 6 and a previous QADM. Increasing the DMADDM mass fraction in NACP nanocomposite increased the antibacterial potency, without compromising the mechanical properties, which matches those of a commercial non-antibacterial composite. The nanocomposite reduced the lactic acid of biofilms by 2 orders of magnitude, and biofilm CFU by 2-3 orders of magnitude. Hence, the novel DMADDM-NACP nanocomposite is

promising for antibacterial and remineralizing restorations to combat secondary caries, the main reason for restoration failure.

## Acknowledgments

We thank Dr. H. Zhou and Dr. A. F. Fouad of the University of Maryland School of Dentistry, and Drs. J. M. Antonucci, N. J. Lin and S. Lin-Gibson of the National Institute of Standards and Technology for discussions and help. We thank Esstech (Essington, PA) for donating the BisGMA and TEGDMA monomers. This study was supported by NIH R01DE17974 (HX), National Natural Science Foundation of China grant 81100745 (LC), the School of Stomatology at the Capital Medical University in China (KZ), and a seed fund (HX) from the University of Maryland School of Dentistry.

## References

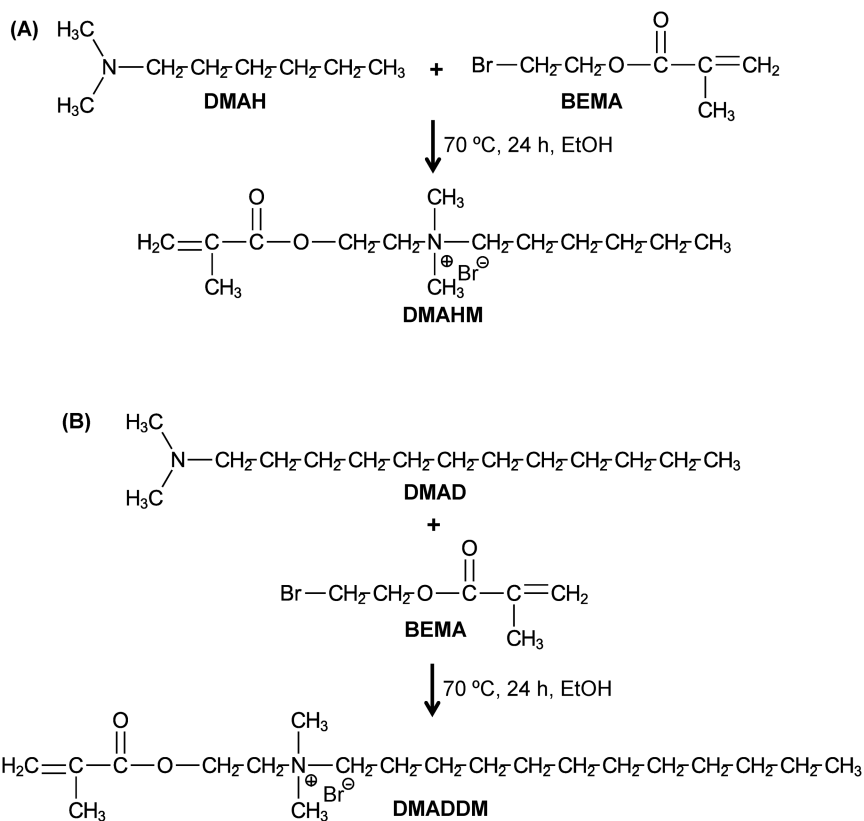
1. Bagramian RA, Garcia-Godoy F, Volpe AR. The global increase in dental caries. A pending public health crisis. *Am J Dent*. 2009; 22:3–8. [PubMed: 19281105]
2. Dye BA, Tan S, Smith V, Lewis BG, Barker LK, Thornton-Evans G, et al. Trends in oral health status: United States, 1988-1994 and 1999-2004. *Vital and Health Statistics*. 2007; 11:1–92. [PubMed: 17633507]
3. Dye BA, Thornton-Evans G. Trends in oral health by poverty status as measured by Healthy People 2010 objectives. *Public Health Reports*. 2010; 125:817–830. [PubMed: 21121227]
4. Mjör IA, Moorhead JE, Dahl JE. Reasons for replacement of restorations in permanent teeth in general dental practice. *International Dent J*. 2000; 50:361–366.
5. Sakaguchi RL. Review of the current status and challenges for dental posterior restorative composites: clinical, chemistry, and physical behavior considerations. *Dent Mater*. 2005; 21:3–6. [PubMed: 15680996]
6. Ferracane JL. Resin composite - State of the art. *Dent Mater*. 2011; 27:29–38. [PubMed: 21093034]
7. Demarco FF, Correa MB, Cenci MS, Moraes RR, Opdam NJM. Longevity of posterior composite restorations: Not only a matter of materials. *Dent Mater*. 2012:87–101. [PubMed: 22192253]
8. Deligeorgi V, Mjor IA, Wilson NH. An overview of reasons for the placement and replacement of restorations. *Prim Dent Care*. 2001; 8:5–11. [PubMed: 11405031]
9. National Institute of Dental and Craniofacial Research (NIDCR) announcement # 13-DE-102. *Dental Resin Composites and Caries*. Mar 5.2009
10. Beazoglou T, Eklund S, Heffley D, Meiers J, Brown LJ, Bailit H. Economic impact of regulating the use of amalgam restorations. *Public Health Rep*. 2007; 122:657–663. [PubMed: 17877313]
11. Saunders RH, Meyerowitz C. Dental caries in older adults. *Dent Clin N Am*. 2005; 49:293–308. [PubMed: 15755406]
12. Bayne SC, Thompson JY, Swift EJ, Stamatiades P, Wilkerson M. A characterization of first-generation flowable composites. *J Am Dent Assoc*. 1998; 129:567–577. [PubMed: 9601169]
13. Ruddell DE, Maloney MM, Thompson JY. Effect of novel filler particles on the mechanical and wear properties of dental composites. *Dent Mater*. 2002; 18:72–80. [PubMed: 11740967]
14. Watts DC, Marouf AS, Al-Hindi AM. Photo-polymerization shrinkage-stress kinetics in resin-composites: methods development. *Dent Mater*. 2003; 19:1–11. [PubMed: 12498890]
15. Ferracane JL. Hygroscopic and hydrolytic effects in dental polymer networks. *Dent Mater*. 2006; 22:211–222. [PubMed: 16087225]
16. Fruits TJ, Knapp JA, Khajotia SS. Microleakage in the proximal walls of direct and indirect posterior resin slot restorations. *Oper Dent*. 2006; 31:719–727. [PubMed: 17153983]
17. Coelho-De-Souza FH, Camacho GB, Demarco FF, Powers JM. Fracture resistance and gap formation of MOD restorations: influence of restorative technique, bevel preparation and water storage. *Oper Dent*. 2008; 33:37–43. [PubMed: 18335731]
18. Drummond JL. Degradation, fatigue, and failure of resin dental composite materials. *J Dent Res*. 2008; 87:710–719. [PubMed: 18650540]

19. Samuel SP, Li S, Mukherjee I, Guo Y, Patel AC, Baran GR, Wei Y. Mechanical properties of experimental dental composites containing a combination of mesoporous and nonporous spherical silica as fillers. *Dent Mater.* 2009; 25:296–301. [PubMed: 18804855]
20. Lim BS, Ferracane JL, Sakaguchi RL, Condon JR. Reduction of polymerization contraction stress for dental composites by two-step light-activation. *Dent Mater.* 2002; 18:436–444. [PubMed: 12098572]
21. Amirouche-Korichi A, Mouzali M, Watts DC. Effects of monomer ratios and highly radiopaque fillers on degree of conversion and shrinkage-strain of dental resin composites. *Dent Mater.* 2009; 25:1411–1418. [PubMed: 19683808]
22. Ritter AV, Swift EJ Jr, Heymann HO, Sturdevant JR, Wilder AD Jr. An eight-year clinical evaluation of filled and unfilled one-bottle dental adhesives. *J Am Dent Assoc.* 2009; 140:28–37. [PubMed: 19119164]
23. Hosoya Y, Shiraishi T, Odatsu T, Nagafuji J, Kotaku M, Miyazaki M, Powers JM. Effects of polishing on surface roughness, gloss, and color of resin composites. *J Oral Sci.* 2011; 53:283–291. [PubMed: 21959654]
24. Zalkind MM, Keisar O, Ever-Hadani P, Grinberg R, Sela MN. Accumulation of *Streptococcus mutans* on light-cured composites and amalgam: An in vitro study. *J Esthet Dent.* 1998; 10:187–190. [PubMed: 9893513]
25. Beyth N, Domb AJ, Weiss EI. An in vitro quantitative antibacterial analysis of amalgam and composite resins. *J Dent.* 2007; 35:201–206. [PubMed: 16996674]
26. Loesche WJ. Role of *Streptococcus mutans* in human dental decay. *Microbiological Reviews.* 1986; 50:353–380. [PubMed: 3540569]
27. Imazato S. Review: Antibacterial properties of resin composites and dentin bonding systems. *Dent Mater.* 2003; 19:449–457. [PubMed: 12837391]
28. Imazato S. Bioactive restorative materials with antibacterial effects: new dimension of innovation in restorative dentistry. *Dent Mater J.* 2009; 28:11–19. [PubMed: 19280964]
29. Li F, Chen J, Chai Z, Zhang L, Xiao Y, Fang M, Ma S. Effects of a dental adhesive incorporating antibacterial monomer on the growth, adherence and membrane integrity of *Streptococcus mutans*. *J Dent.* 2009; 37:289–296. [PubMed: 19185408]
30. Xie D, Weng Y, Guo X, Zhao J, Gregory RL, Zheng C. Preparation and evaluation of a novel glass-ionomer cement with antibacterial functions. *Dent Mater.* 2011; 27:487–496. [PubMed: 21388668]
31. He J, Söderling E, Lassila LV, Vallittu PK. Incorporation of an antibacterial and radiopaque monomer in to dental resin system. *Dent Mater.* 2012; 28:e110–e117. [PubMed: 22575737]
32. Antonucci JM, Zeiger DN, Tang K, Lin-Gibson S, Fowler BO, Lin NJ. Synthesis and characterization of dimethacrylates containing quaternary ammonium functionalities for dental applications. *Dent Mater.* 2012; 28:219–228. [PubMed: 22035983]
33. Imazato S, Kinomoto Y, Tarumi H, Ebisu S, Tay FR. Antibacterial activity and bonding characteristics of an adhesive resin containing antibacterial monomer MDPB. *Dent Mater.* 2003; 19:313–319. [PubMed: 12686296]
34. Imazato S, Tay FR, Kaneshiro AV, Takahashi Y, Ebisu S. An in vivo evaluation of bonding ability of comprehensive antibacterial adhesive system incorporating MDPB. *Dent Mater.* 2007; 23:170–176. [PubMed: 16469372]
35. Xu X, Wang Y, Liao S, Wen ZT, Fan Y. Synthesis and characterization of antibacterial dental monomers and composites. *J Biomed Mater Res.* 2012; 100B:1511–1162.
36. Weng Y, Howard L, Guo X, Chong VJ, Gregory RL, Xie D. A novel antibacterial resin composite for improved dental restoratives. *J Mater Sci Mater Med.* 2012; 23:1553–1561. [PubMed: 22466818]
37. Skrtic D, Hailer AW, Takagi S, Antonucci JM, Eanes ED. Quantitative assessment of the efficacy of amorphous calcium phosphate/methacrylate composites in remineralizing caries-like lesions artificially produced in bovine enamel. *J Dent Res.* 1996; 75:1679–1686. [PubMed: 8952621]
38. Dickens SH, Flaim GM, Takagi S. Mechanical properties and biochemical activity of remineralizing resin-based Ca-PO<sub>4</sub> cements. *Dent Mater.* 2003; 19:558–566. [PubMed: 12837405]

39. Langhorst SE, O'Donnell JNR, Skrtic D. In vitro remineralization of enamel by polymeric amorphous calcium phosphate composite: Quantitative microradiographic study. *Dent Mater.* 2009; 25:884–891. [PubMed: 19215975]
40. Skrtic D, Antonucci JM, Eanes ED, Eichmiller FC, Schumacher GE. Physiological evaluation of bioactive polymeric composites based on hybrid amorphous calcium phosphates. *J Biomed Mater Res.* 2000; 53B:381–391. [PubMed: 10898879]
41. Xu HHK, Weir MD, Sun L. Calcium and phosphate ion releasing composite: Effect of pH on release and mechanical properties. *Dent Mater.* 2009; 25:535–542. [PubMed: 19101026]
42. Xu HHK, Moreau JL. Dental glass-reinforced composite with calcium and phosphate ion release for caries inhibition. *J Biomed Mater Res.* 2010; 92B:332–340.
43. Xu HHK, Weir MD, Sun S, Moreau JL, Takagi S, Chow LC, Antonucci JM. Strong nanocomposites with Ca, PO<sub>4</sub> and F release for caries inhibition. *J Dent Res.* 2010; 89:19–28. [PubMed: 19948941]
44. Moreau JL, Sun L, Chow LC, Xu HHK. Mechanical and acid neutralizing properties and inhibition of bacterial growth of amorphous calcium phosphate dental nanocomposite. *J Biomed Mater Res.* 2011; 98B:80–88.
45. Xu HHK, Moreau JL, Sun L, Chow LC. Nanocomposite containing amorphous calcium phosphate nanoparticles for caries inhibition. *Dent Mater.* 2011; 27:762–769. [PubMed: 21514655]
46. Moreau JL, Weir MD, Giuseppetti AA, Chow LC, Antonucci JM, Xu HHK. Long-term mechanical durability of dental nanocomposites containing amorphous calcium phosphate nanoparticles. *J Biomed Mater Res B.* 2012; 100:1264–73.
47. Melo MAS, Weir MD, Rodrigues LKA, Xu HHK. Novel calcium phosphate nanocomposite with caries-inhibition in a human in situ model. *Dent Mater.* 2012 in review.
48. Weir MD, Chow LC, Xu HHK. Remineralization of demineralized enamel via calcium phosphate nanocomposite. *J Dent Res.* 2012 accepted for publication.
49. Cheng L, Weir MD, Xu HHK, Antonucci JM, Kraigsley AM, Lin NJ, Lin-Gibson S, Zhou XD. Antibacterial amorphous calcium phosphate nanocomposite with quaternary ammonium salt and silver nanoparticles. *Dent Mater.* 2012; 28:561–572. [PubMed: 22305716]
50. Cheng L, Weir MD, Zhang K, Xu SM, Chen Q, Zhou XD, Xu HHK. Antibacterial nanocomposite with calcium phosphate and quaternary ammonium. *J Dent Res.* 2012; 91:460–466. [PubMed: 22403412]
51. Imazato S, Kuramoto A, Takahashi Y, Ebisu S, Peters MC. In vitro antibacterial effects of the dentin primer of Clearfil Protect Bond. *Dent Mater.* 2006; 22:527–532. [PubMed: 16198404]
52. Huang L, Xiao YH, Xing XD, Li F, Ma S, Qi LL, Chen JH. Antibacterial activity and cytotoxicity of two novel cross-linking antibacterial monomers on oral pathogens. *Arch Oral Biol.* 2011; 56:367–373. [PubMed: 21074143]
53. Chow LC, Sun L, Hockey B. Properties of nanostructured hydroxyapatite prepared by a spray drying technique. *J Res NIST.* 2004; 109:543–551.
54. Cheng L, Zhang K, Melo MAS, Weir MD, Zhou XD, Xu HHK. Anti-biofilm dentin primer with quaternary ammonium and silver nanoparticles. *J Dent Res.* 2012; 91:598–604. [PubMed: 22492276]
55. McBain AJ. In vitro biofilm models: an overview. *Adv Appl Microbiol.* 2009; 69:99–132. [PubMed: 19729092]
56. Zhang K, Melo MAS, Cheng L, Weir MD, Bai YX, Xu HHK. Effect of quaternary ammonium and silver nanoparticle-containing adhesives on dentin bond strength and dental plaque microcosm biofilms. *Dent Mater.* 2012; 28:842–852. [PubMed: 22592165]
57. Lima JP, Sampaio de Melo MA, Borges FM, Teixeira AH, Steiner-Oliveira C, Nobre Dos Santos M, et al. Evaluation of the antimicrobial effect of photodynamic antimicrobial therapy in an in situ model of dentine caries. *Eur J Oral Sci.* 2009; 117:568–74. [PubMed: 19758254]
58. Park JH, Tanabe Y, Tinanoff N, Turng BF, Lilli H, Minah GE. Evaluation of microbiological screening systems using dental plaque specimens from young children aged 6-36 months. *Caries Res.* 2006; 40:277–80. [PubMed: 16707879]
59. Imazato S, Torii M, Tsuchitani Y, McCabe JF, Russell RRB. Incorporation of bacterial inhibitor into resin composite. *J Dent Res.* 1994; 73:1437–1443. [PubMed: 8083440]

60. Beyth N, Yudovin-Farber I, Bahir R, Domb AJ, Weiss EI. Antibacterial activity of dental composites containing quaternary ammonium polyethylenimine nanoparticles against *Streptococcus mutans*. *Biomaterials*. 2006; 27:3995–4002. [PubMed: 16564083]
61. Namba N, Yoshida Y, Nagaoka N, Takashima S, Matsuura-Yoshimoto K, Maeda H, Van Meerbeek B, Suzuki K, Takashida S. Antibacterial effect of bactericide immobilized in resin matrix. *Dent Mater*. 2009; 25:424–430. [PubMed: 19019421]
62. Tiller JC, Liao CJ, Lewis K, Klibanov AM. Designing surfaces that kill bacteria on contact. *Proc Natl Acad Sci USA*. 2001; 98:5981–5. [PubMed: 11353851]
63. Murata H, Koepsel RR, Matyjaszewski K, Russell AJ. Permanent, non-leaching antibacterial surfaces -2: How high density cationic surfaces kill bacterial cells. *Biomaterials*. 2007; 28:4870–9. [PubMed: 17706762]
64. Imazato S, Ebi N, Tarumi H, Russell RR, Kaneko T, Ebisu S. Bactericidal activity and cytotoxicity of antibacterial monomer MDPB. *Biomaterials*. 1999; 20:899–903. [PubMed: 10226716]
65. Beyth N, Yudovin-Farber I, Perez-Davidi M, Domb AJ, Weiss EI. Polyethyleneimine nanoparticles incorporated into resin composite cause cell death and trigger biofilm stress in vivo. *Proc Natl Acad Sci USA*. 2010; 107:22038–43. [PubMed: 21131569]
66. Li F, Weir MD, Fouad AF, Xu HHK. Effect of salivary pellicle on antibacterial activity of novel antibacterial dental adhesives using a dental plaque microcosm biofilm model. *Dent Mater*. submitted in November 2012, in review.



**Figure 1.**

A modified Menshutkin reaction was used to synthesize new antibacterial monomers: (A) DMAHM, and (B) DMADDM. DMAH = N,N-dimethylaminohexane. BEMA = 2-bromoethyl methacrylate. DMAHM = dimethylaminohexane methacrylate. DMAD = 1-(dimethylamino)docecane. DMADDM = dimethylaminododecyl methacrylate. EtOH = anhydrous ethanol. The number of the alkyl chain length units was 6 for DMAHM and 12 for DMADDM.

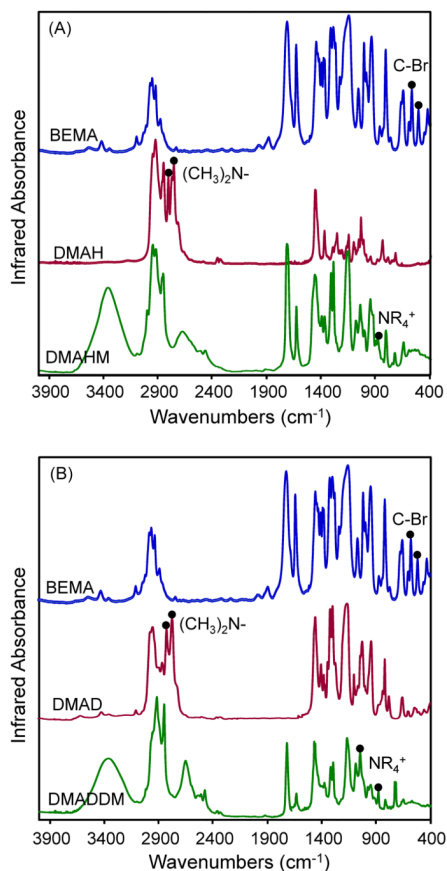


**Figure 2.**

FTIR spectra of reactants and products for: (A) DMAHM, and (B) DMADDM. The characterization using FTIR indicated that the Menshutkin reaction was successful. The infrared spectroscopy showed the disappearance of C-Br and tertiary amine groups, and the appearance of quaternary ammonium group that resulted from the reaction. In each plot, the appearance of the NR<sub>4</sub><sup>+</sup> peak in the last curve corresponded to the formation of the quaternary ammonium group.

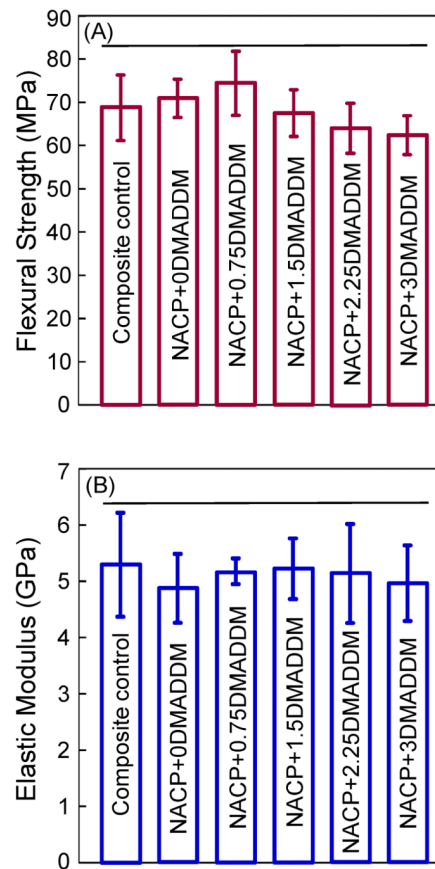


**Figure 3.** Mechanical properties of composites: (A) flexural strength, and (B) elastic modulus (mean  $\pm$  sd; n = 6). NACP+0DMADDM refers to NACP nanocomposite containing 0% DMADDM; NACP+0.75DMADDM refers to NACP nanocomposite containing 0.75% of DMADDM; and so on. Adding up to 3% of DMADDM into NACP nanocomposite resulted in no significant decrease in strength and elastic modulus. Horizontal line indicates values that are not significantly different from each other ( $p > 0.1$ ).

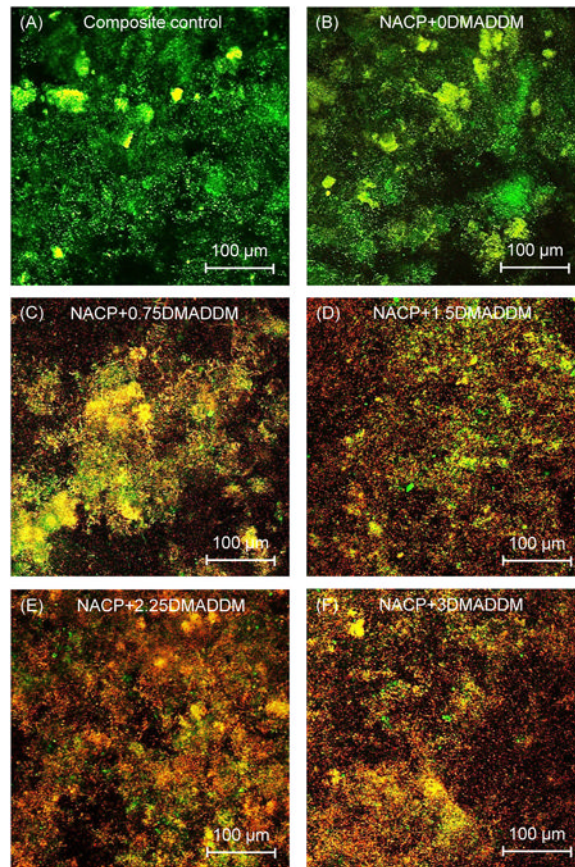


**Figure 4.**

Typical confocal laser scanning microscopy (CLSM) images of live/dead stained biofilms on composites. Live bacteria were stained green, and dead bacteria were stained red. Live/dead bacteria that were close to, or on the top of, each other produced yellow/orange colors. Composite control and NACP nanocomposite had primarily live bacteria. The DMADDM-containing nanocomposites showed substantial antibacterial activity.

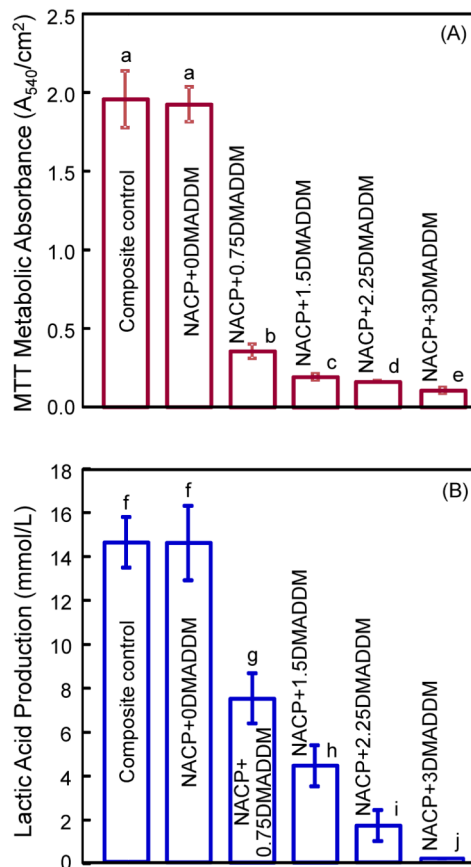


**Figure 5.** Dental plaque microcosm biofilms adherent on composites: (A) MTT metabolic activity, and (B) lactic acid production (mean  $\pm$  sd;  $n = 6$ ). NACP+0DMADDM refers to NACP nanocomposite containing 0% DMADDM; NACP+0.75DMADDM refers to NACP nanocomposite containing 0.75% of DMADDM; and so on. In each plot, values with dissimilar letters are significantly different ( $p < 0.05$ ).



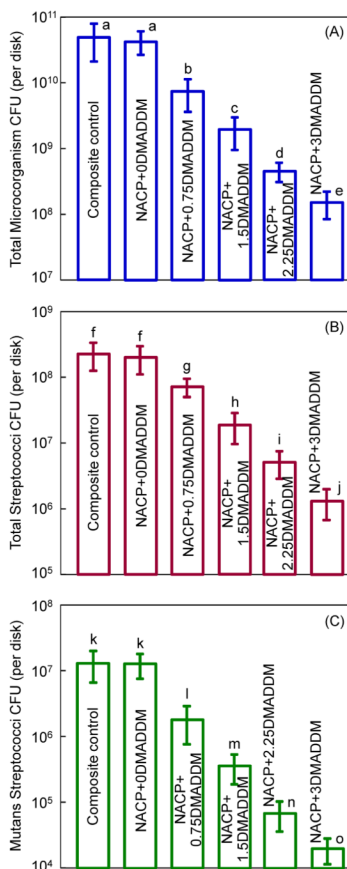


**Figure 6.** Colony-forming unit (CFU) counts for: (A) Total microorganisms, (B) total streptococci, and (C) mutans streptococci (mean ± sd; n = 6). NACP+0DMADDM refers to NACP nanocomposite containing 0% DMADDM; NACP+0.75DMADDM refers to NACP nanocomposite containing 0.75% of DMADDM; and so on. In each plot, values with dissimilar letters are significantly different (p < 0.05). Note the log scale for the y-axis.

**Table 1**  
**MIC and MBC values of various antibacterial agents against *S. mutans*\***

Compound	MBC	MIC
QADM	$2.5 \times 10^4$ $\mu\text{g/mL}$	$1.25 \times 10^4$ $\mu\text{g/mL}$
DMAHM	$3.13 \times 10^3$ $\mu\text{g/mL}$	$1.56 \times 10^3$ $\mu\text{g/mL}$
DMADDM	12.21 $\mu\text{g/mL}$	6.10 $\mu\text{g/mL}$
CHX	3.91 $\mu\text{g/mL}$	1.95 $\mu\text{g/mL}$

\* CHX = Chlorhexidine. QADM = quaternary ammonium dimethacrylate. DMAHM = dimethylaminohexane methacrylate. DMADDM = dimethylaminododecyl methacrylate. Tests were repeated in triplicate, and all three repeats yielded the same value.